Variations in the Drought Severity Index in Response to Climate Change on the Tibetan Plateau

WANG Xiangtao[1, 2], ZHANG Xianzhou[1, 2, 3], WANG Junhao[1, 2], NIU Ben[1, 2, *]

1. Lhasa Plateau Ecosystem Research Station, Key Laboratory of Ecosystem Network Observation and Modeling, Institute of Geographic Sciences and Natural Resources Research, Chinese Academy of Sciences, Beijing 100101, China;
2. University of Chinese Academy of Sciences, Beijing 100049, China;
3. College of Resources and Environment, University of Chinese Academy of Sciences, Beijing 100190, China

Abstract: Quantifying the relationship between the drought severity index and climate factors is crucial for predicting drought risk in situations characterized by climate change. However, variations in drought risk are not readily discernible under conditions of climate change, and this is particularly the case on the Tibetan Plateau. This study examines the correlations between the annual drought severity index (DSI) and 14 climate factors (including temperature, precipitation, humidity, wind speed, and hours of sunshine factors), on the Tibetan Plateau from 2000 to 2011. Spatial average DSI increased with precipitation and minimum relative humidity, while it decreased as the hours of sunshine increased. The correlation between DSI and climate factors varied with vegetation types. In alpine meadows, the correlation of the spatial DSI average with the percentage of sunshine and hours of sunshine (*P*<0.001) was higher compared to that in alpine steppes (*P*<0.05). Similarly, average vapor pressure and minimum relative humidity had significant positive effects on spatial DSI in alpine meadows, but had insignificant effects in alpine steppes. The magnitude of DSI change correlated negatively with temperature, precipitation, and vapor pressure, and positively with wind speed and sunshine. This demonstrates that the correlation between drought and climate change on the Tibetan Plateau is dependent on the type of ecosystem.

Key words: alpine ecosystems; climate change; drought; Tibetan Plateau

1 Introduction

Drought is an important climate event and is linked to water availability, temperature, sunshine, and wind speed (Dai, 2011; Trenberth et al., 2014). Generally, water availability plays an important role in terrestrial ecosystems, and drought has an adverse effect on vegetation growth (Mu et al., 2013; Wang et al., 2013). Several studies have focused on how drought changes under climate change. However, neither modeling nor observations provide a widely accepted answer to the question of how climate change impacts drought (Sheffield et al., 2012; Dai, 2013; Trenberth et al., 2014). Understanding the relationship between drought and changes in climate factors is crucial for predicting future

changes in aridity and coping with drought-related issues.

The Tibetan Plateau is one of the landscapes considered to be sensitive to climate change (IPCC, 2013; Li et al., 2019). Approximately two-thirds of the Tibetan Plateau is covered with arid and semiarid alpine ecosystems that are expected to become much drier as global warming continues (Seager et al., 2010). Therefore, alpine ecosystems on the Tibetan Plateau are likely to endure more extreme warming than biomes elsewhere (IPCC, 2013). It is predicted that global warming will exacerbate drought severity in the future (Trenberth et al., 2014). Several recent studies have also indicated that the decreased magnitude of soil moisture in in-situ experiments is due to the magnitude of increase in

soil temperature (Shen et al., 2016; Zhong et al., 2016; Yu et al., 2019b). These findings imply that drought risk may be more extensive, and its magnitude may be greater on the Tibetan Plateau compared to other regions of the world. For example, Wang and Chen (2014) have found that drought risk on the Tibetan Plateau is much higher than it is on average in other parts of China.

The impact of climate change varies across different vegetation types on the Tibetan Plateau (Fu et al., 2016). To the best of our knowledge, there is an absence of research that examines correlations between inter-annual variations of the drought index and climate change across vegetation types on the Tibetan Plateau. Moreover, previous studies of the Tibetan Plateau have focused mainly on the correlation of the drought index with temperature and precipitation and not considered other climate factors (e.g., vapor pressure, relative humidity, wind speed and hours of sunshine) (Liu et al., 2014; Yang et al., 2014). Recently, the Moderate Resolution Imaging Spectroradiometer (MODIS) introduced a new drought index called the drought severity index (DSI) that uses MODIS-derived actual and potential evapotranspiration, and the normalized difference vegetation index (NDVI) (Mu et al., 2013). This index facilitates analyses of drying conditions and relationships associated with climate factors at a global or regional scale. In this study, we used MODIS DSI data and meteorological data to: 1) analyze and compare inter-annual variations of DSI and their relationships with climate factors across key alpine ecosystems; and 2) examine whether global warming has a negative effect on the DSI of the Tibetan Plateau.

2 Materials and methods

2.1 Study area

Known as the Third Pole by some, the Tibetan Plateau has distinctive features including high elevation (elevation >4000 m), strong solar radiation, thin air and low temperatures. The predominant vegetation types include alpine meadows, alpine steppes, temperate steppes, forests, shrublands, and croplands.

2.2 Drought severity index (DSI) data

The vegetation response-incorporated DSI products used in this study were obtained from MODIS16 onboard the NASA Earth Observing System (EOS) Terra and Aqua satellites. The MODIS 16 evapotranspiration (ET) and potential evapotranspiration (PET) data were used as primary inputs to calculate the DSI; the spatial resolution was 0.05°×0.05° and the temporal resolution was one year. The specific calculation follows Mu et al. (2013); the ratio of ET to PET is shown in Eq. (1):

$$Ratio = ET / PET \tag{1}$$

The temporal standard deviation of ratio (σ_{Ratio}) and ratio average ($\overline{Ratio}$) were then computed on a grid cell-wise basis over the available satellite record (from 2000 to present). The standardized ratio (Z_{Ratio}) was then calculated as:

$$Z_{Ratio} = (Ratio - \overline{Ratio}) / \sigma_{Ratio} \tag{2}$$

We derived the standardized NDVI (Z_{NDVI}) for each composite period during the classified growing season at each grid cell as:

$$Z_{NDVI} = (NDVI - \overline{NDVI}) / \sigma_{NDVI} \tag{3}$$

The Z_{Ratio} and Z_{NDVI} terms were then summed as:

$$Z = Z_{Ratio} + Z_{NDVI} \tag{4}$$

The remotely sensed DSI was finally calculated as the standardized Z value:

$$DSI = Z - \overline{Z} / \sigma_z \tag{5}$$

Compared to traditional drought monitoring methods, DSI enhances the capability of near real-time drought monitoring (Mu et al., 2013). In addition, DSI is associated with the remote-sensing net primary productivity of vegetation (NPP). DSI and NPP can be used together to evaluate the interaction between water supply and ecosystems, including the effects of drought on crop yields and forest productivity (Atkinson et al., 2011). This can assist in regional drought assessment and the timely and effective development of drought mitigation strategies.

2.3 Climate data

We obtained climate data from the China Meteorological Data Sharing Service System (http://cdc.cma.gov.cn/). The study used data from a total of 69 meteorological stations. Of these stations, 22 stations were in alpine meadows, 8 in alpine steppes, 4 in temperate steppes, 7 in forests, 12 in shrublands and 16 in croplands. Climate data included five temperature factors (average annual air temperature (Ta), maximum air temperature (MAT), minimum air temperature (MIT), extreme maximum air temperature (EMAT), and extreme minimum air temperature (EMIT)), two precipitation factors (total annual precipitation (TP), and maximum precipitation (MAP)), four humidity factors (average annual vapor pressure (Ea), relative humidity (RH), minimum relative humidity (MIRH), and vapor pressure deficit (VPD)), two sunshine factors (annual percentage of sunshine (SP) and total sunshine hours (SH)), and average annual wind speed (WS).

2.4 Data analysis

The map for vegetation type (1:1000000 scale) was converted into a raster file (0.05°×0.05° spatial resolution) prior to other analyses. We used the slope and intercept of the regression straight line to analyze changes in DSI and the five temperature factors, two precipitation factors, four humidity factors, two sunshine factors, and annual average wind speed. We used a correlation analysis to analyze the relationship between DSI and the climate factors. All spatial analyses were performed using ArcGIS (version 9.3).

3   Results and discussion

3.1   Climate factor changes

The climate became warmer and drier from 2000 to 2011,

based on meteorological records for the Tibetan Plateau (Fig. 1). Specifically, average Ta, MAT, and MIT increased by 0.07, 0.09 and 0.07 ℃ yr^{-1}, respectively. Spatially, average MAP and VPD showed increasing trends of 0.33 mm yr^{-1}
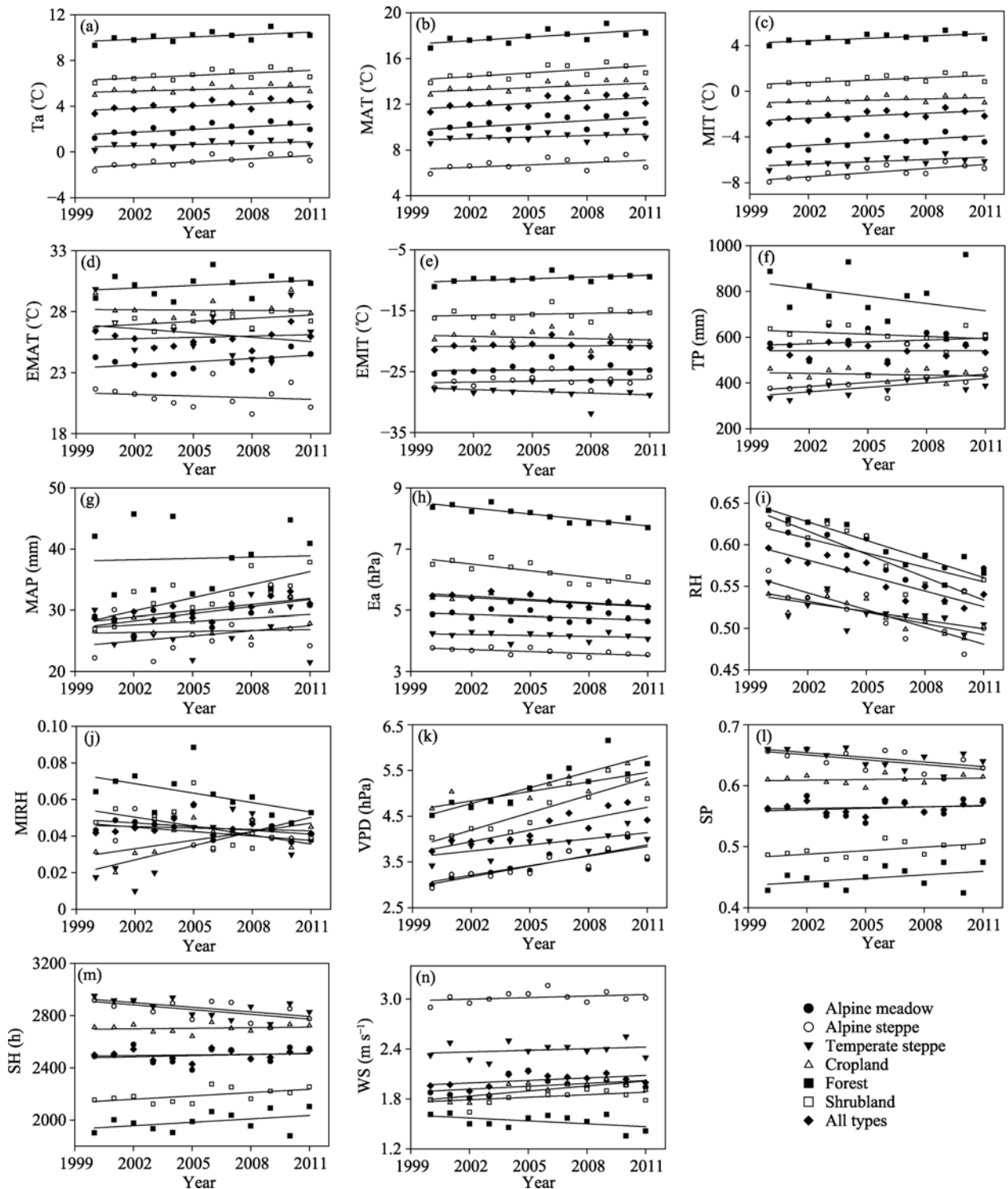

Fig. 1   Linear trends for (a) Ta, average annual air temperature; (b) MAT, maximum air temperature; (c) MIT, minimum air temperature; (d) EMAT, extreme maximum air temperature; (e) EMIT, extreme minimum air temperature; (f) TP, total precipitation; (g) MAP, maximum precipitation; (h) Ea, average vapor pressure; (i) RH, average relative humidity; (j) MIRH, minimum relative humidity; (k) VPD, average vapor pressure deficit; (l) SP, percentage of sunshine; (m) SH, sunshine hours; and (n) WS, average wind speed; from 2000 to 2011 based on data from 69 meteorological stations on the Tibetan Plateau.

and 0.01 hPa yr^{-1}, while Ea and RH decreased by -0.04 hPa yr^{-1} and -0.01 hPa yr^{-1}. However, climate changes varied with vegetation type (Fig.1), a finding consistent with those of previous studies (Fu et al., 2016; Shen et al., 2014). The climate showed warming and drying trends from 2000 to 2011 at meteorological stations in alpine meadows, alpine steppes, forests, and shrublands. However, meteorological stations in temperate steppes and croplands showed only a drying trend. Additionally, it became dimmer in alpine steppes and temperate steppes, and brighter in shrublands, based on data for the percentage of sunshine and sunshine hours (Fig. 1).

3.2 DSI changes

Spatially averaged DSI change varied among vegetation types (Fig. 2). Forests were the only vegetation type to experience a decrease in spatially averaged DSI with a rate of -0.039 yr^{-1}. The DSI for other vegetation types increased in recent years. This was mainly because the largest magnitude of TP decreased and VPD increased among the six vegetation types.
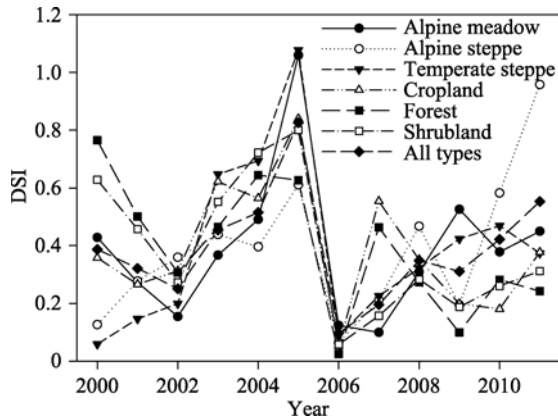

Fig. 2   Linear trends for the annual drought severity index (DSI) from 2000 to 2011, for different vegetation types on the Tibetan Plateau

Inter-annual DSI change during recent years varied among the 69 meteorological stations (Fig. 3). Eight stations showed a decrease, with rates from -0.13 to -0.09 yr^{-1}. In contrast, only the Wudaoliang station had an increase with a rate of 0.10 yr^{-1}. This finding was consistent with previous studies which indicated that changes of water availability had varied from station to station on the Tibetan Plateau in recent years (Sun et al., 2013; Shen et al., 2014). Overall, the southern Tibetan Plateau showed a drying trend, while the northern Tibetan Plateau showed a wetting trend (Fig. 3). This finding is consistent with previous studies (Wang et al., 2013; Zhang et al., 2013).

The change rate of DSI decreased with increasing temperatures (i.e., Ta, MAT, MIT, EMAT, and EMIT), and environmental humidity (TP, MAP, and Ea), but increased with increasing SP, SH, and WS (Fig. 4). These findings indicate that DSI was more responsive to warming in colder environments, to water availability in drier environments and

to sunshine conditions in more brightly lit environments. Therefore, clarifying the correlation between DSI and water availability requires consideration of local climate conditions.
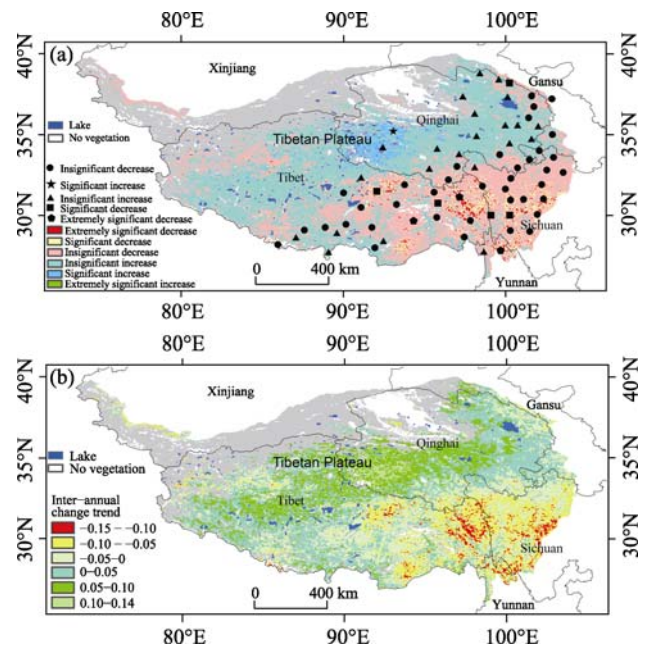

Fig. 3   Drought severity index trend from 2000 to 2011 on the Tibetan Plateau

DSI change showed a positive relationship with TP change, but negative correlations with temperature (MAT, EMAT, EMIT), SP and SH changes (Fig. 5). Likewise, recent studies found that higher experimental warming resulted in greater environmental drying (Li et al., 2011; Yu et al., 2019b). These findings indicate that the magnitude of warming and water availability had opposite effects on changes to DSI. Additionally, the negative effect of changes to sunshine conditions on DSI dampened the positive effect of the change of water availability on DSI (Fig. 5). Changes to climate factors and background values differed among the six vegetation types and among the 69 meteorological stations (Fig. 1, Fig. 6, Fig. 7, Fig. 8). This evidence suggests that inter-annual DSI variations may be attributed to changes in climate factors and changes in the background values of climate factors among the six vegetation types or among the 69 meteorological stations. For example, in winter, the land cover of different vegetation types can vary greatly. There can be evergreen plants in forests and winter crops in croplands. In addition, canopy coverages can change with vegetation types (Shen et al., 2014). Dense canopy often has higher transpiration and lower soil moisture, while shielding against incident solar radiation and soil longwave radiation (Sun and Kafatos, 2007; Kerchove et al., 2013).

Thus, the findings in our study suggest that the correlations between DSI change and climate factors are dependent on local climate conditions.
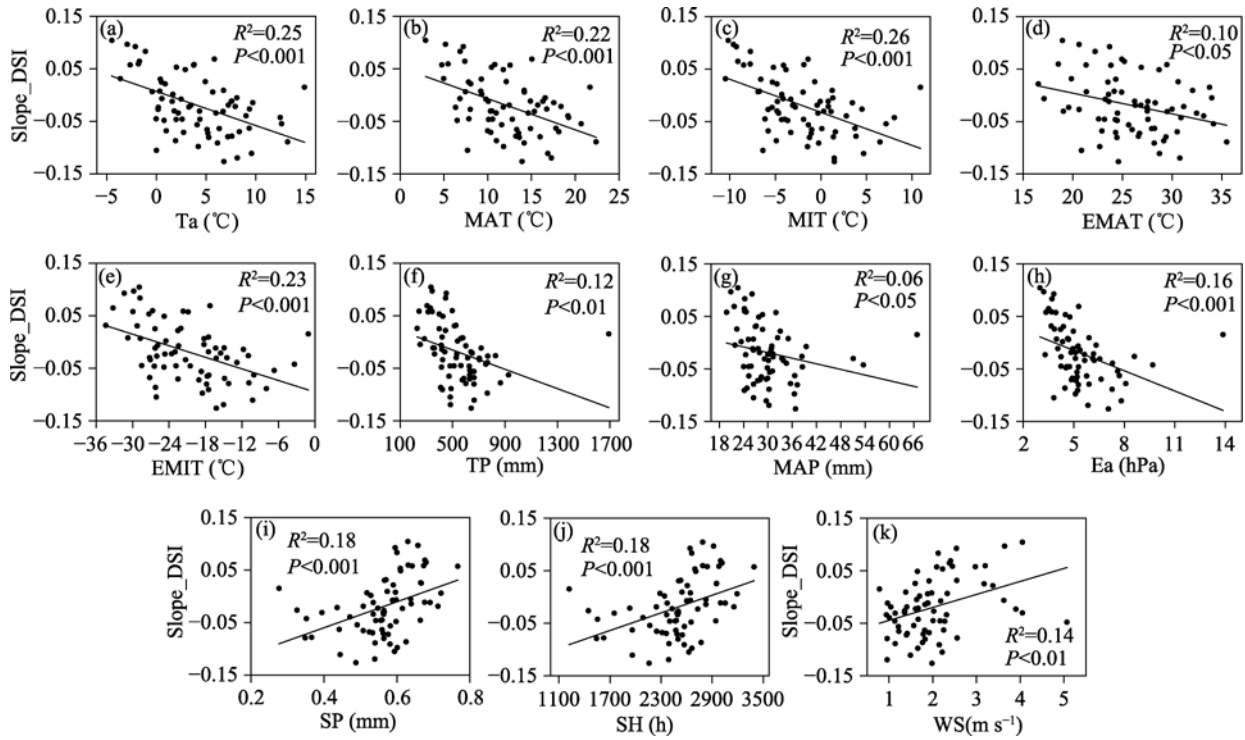
Fig. 4   Relationships of the linear trend of the annual drought severity index (Slope_DSI) with climate variables on the Tibetan Plateau. (a) average annual temperature (Ta); (b) maximum annual temperature (MAT); (c) minimum annual temperature (MIT); (d) extreme maximum annual temperature (EMAT); (e) extreme minimum annual temperature (EMIT); (f) annual precipitation (TP); (g) maximum annual precipitation (MAP); (h) average annual vapor pressure (Ea); (i) annual sunshine percentage (SP); (j) annual sunshine hours (SH); and (k) average annual wind speed (WS).
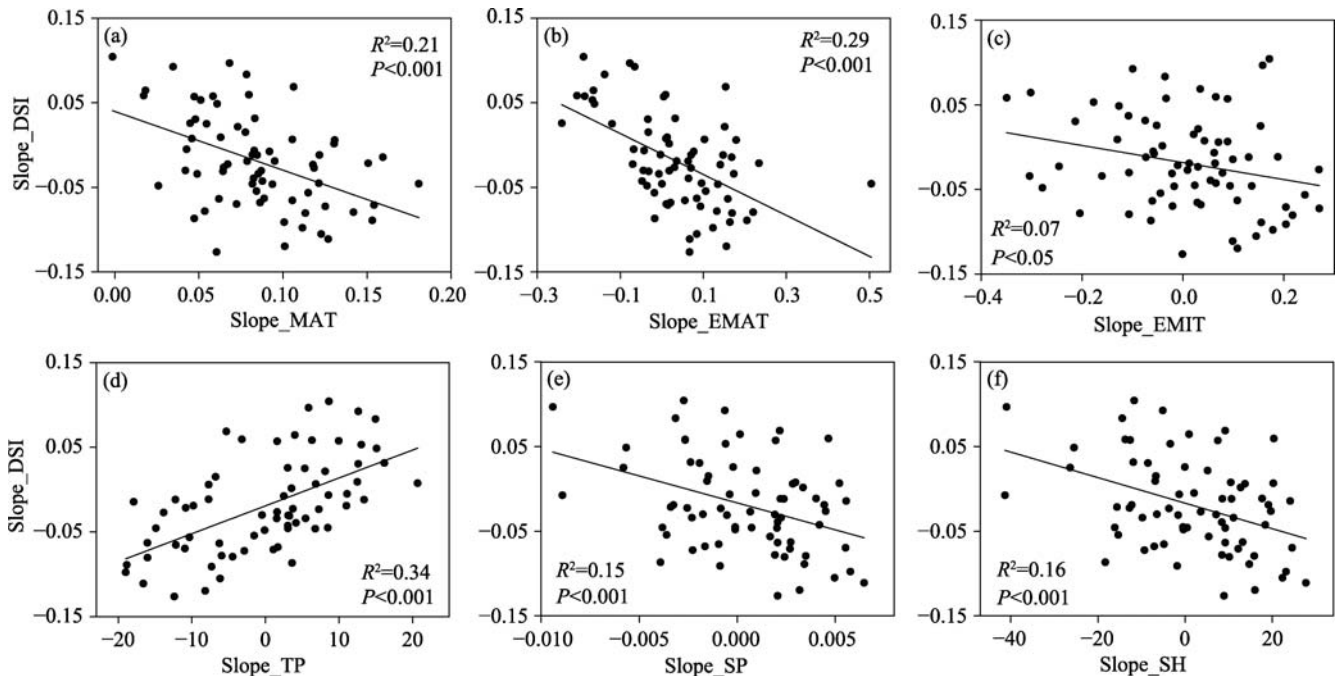

Fig. 5   Relationships between the linear trend of the annual drought severity index (Slope_DSI) and the linear trends of several climate factors: (a) maximum annual temperature (Slope_MAT); (b) extreme maximum annual temperature (Slope_EMAT); (c) extreme minimum annual temperature (Slope_EMIT); (d) annual precipitation (Slope_TP); (e) annual sunshine percentage (Slope_SP); and (f) annual sunshine hours (Slope_SH).
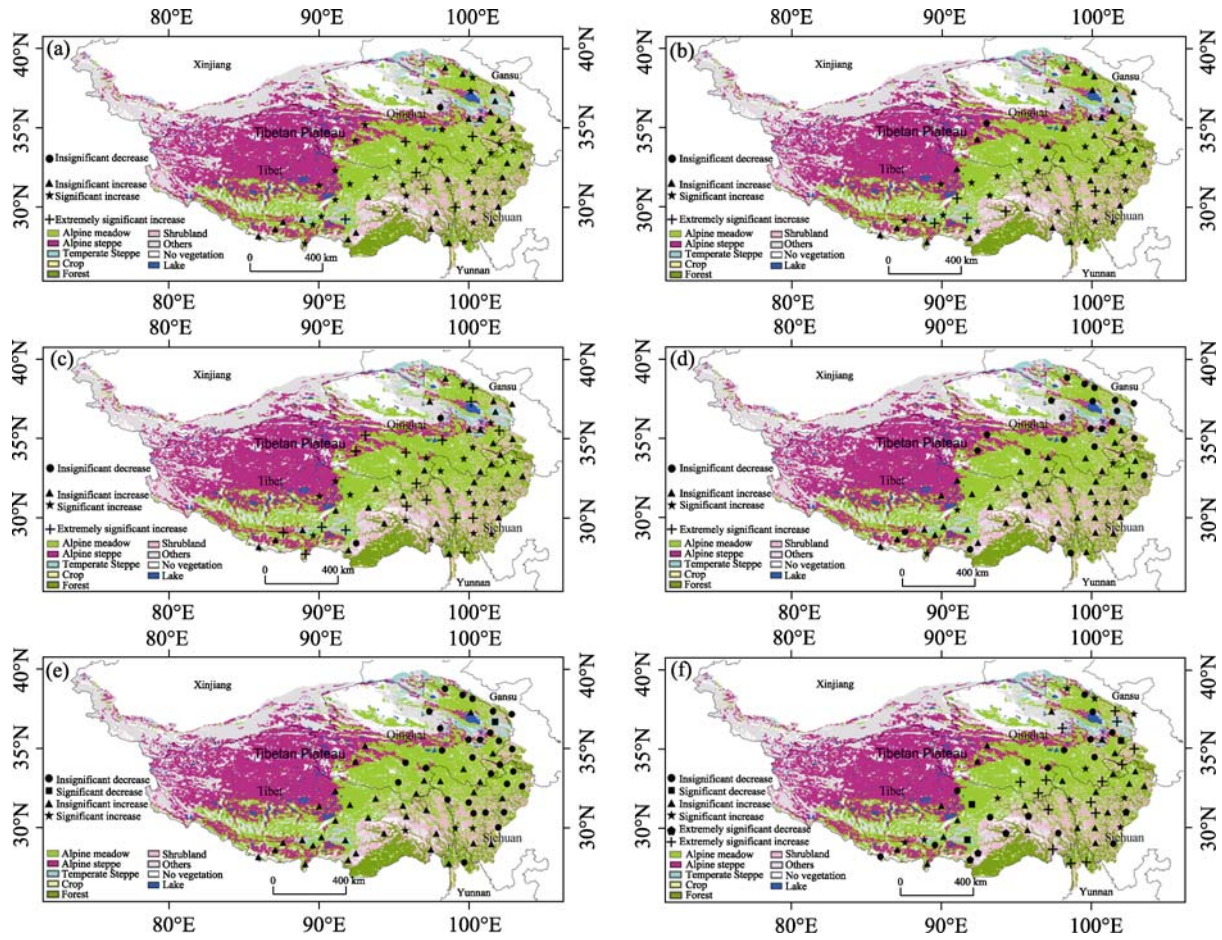
Fig. 6   Annual trends for (a) Ta, average air temperature; (b) MAT, maximum air temperature; (c) MIT, minimum air temperature; (d) EMAT, extreme maximum air temperature; (e) EMIT, extreme minimum air temperature; (f) WS, average wind speed; from 2000 to 2011 at 69 meteorological stations on the Tibetan Plateau.

3.3   Relationships between DSI and climate factors

Spatially averaged DSI was related positively to spatially averaged TP and MIRH, but correlated negatively to SP and

SH at all of the 69 meteorological stations (Table 1). Therefore, DSI can mirror water availability conditions, and it is likely that the increase in sunshine resulted in drying around all of the meteorological stations (Mu et al., 2013).

Table 1   Correlation coefficients for spatially averaged annual drought severity index (DSI) with spatially averaged climate factors from 2000 to 2011 at 69 meteorological stations on the Tibetan Plateau

Types	Ta	MAT	MIT	EMAT	EMIT	TP	MAP	Ea	RH	MIRH	VPD	SP	SH	WS
Alpine meadows	−0.11	−0.42	0.26	−0.43	−0.08	0.59*	0.20	0.67*	0.50	0.71**	−0.35	−0.85***	−0.87***	0.49
Alpine steppes	0.28	−0.07	0.58*	−0.36	0.20	0.70*	0.19	0.07	−0.17	−0.35	0.23	−0.74**	−0.74**	0.19
Temperate steppes	0.20	0.10	0.25	0.04	0.57	0.42	−0.19	0.29	−0.16	0.07	0.34	−0.23	−0.19	0.18
Croplands	−0.34	−0.48	−0.14	−0.55	−0.05	0.43	−0.22	0.36	0.50	0.26	−0.49	−0.90***	−0.91***	0.26
Forests	−0.71**	−0.77**	−0.73**	−0.63*	−0.69*	0.54	0.24	0.74**	0.78**	−0.04	−0.76**	−0.66*	−0.65*	−0.02
Shrublands	−0.66*	−0.78**	−0.51	−0.61*	−0.36	0.66*	−0.43	0.69*	0.75**	0.83***	−0.73**	−0.75**	−0.75**	0.03
All types	−0.28	−0.49	−0.03	−0.40	−0.11	0.61*	−0.18	0.54	0.50	0.74**	−0.42	−0.86***	−0.86***	0.31

Note: Ta, average annual temperature; MAT, maximum temperature; MIT, minimum temperature; EMAT, extreme maximum temperature; EMIT, extreme minimum temperature; TP, total precipitation; MAP, maximum precipitation; Ea, average vapor pressure; RH, average relative humidity; MIRH, minimum relative humidity; VPD, average vapor pressure deficit; SP, percentage of sunshine; SH, sunshine hours; WS, wind speed. The *, ** and *** indicate $P < 0.05$, $P < 0.01$ and $P < 0.001$, respectively.
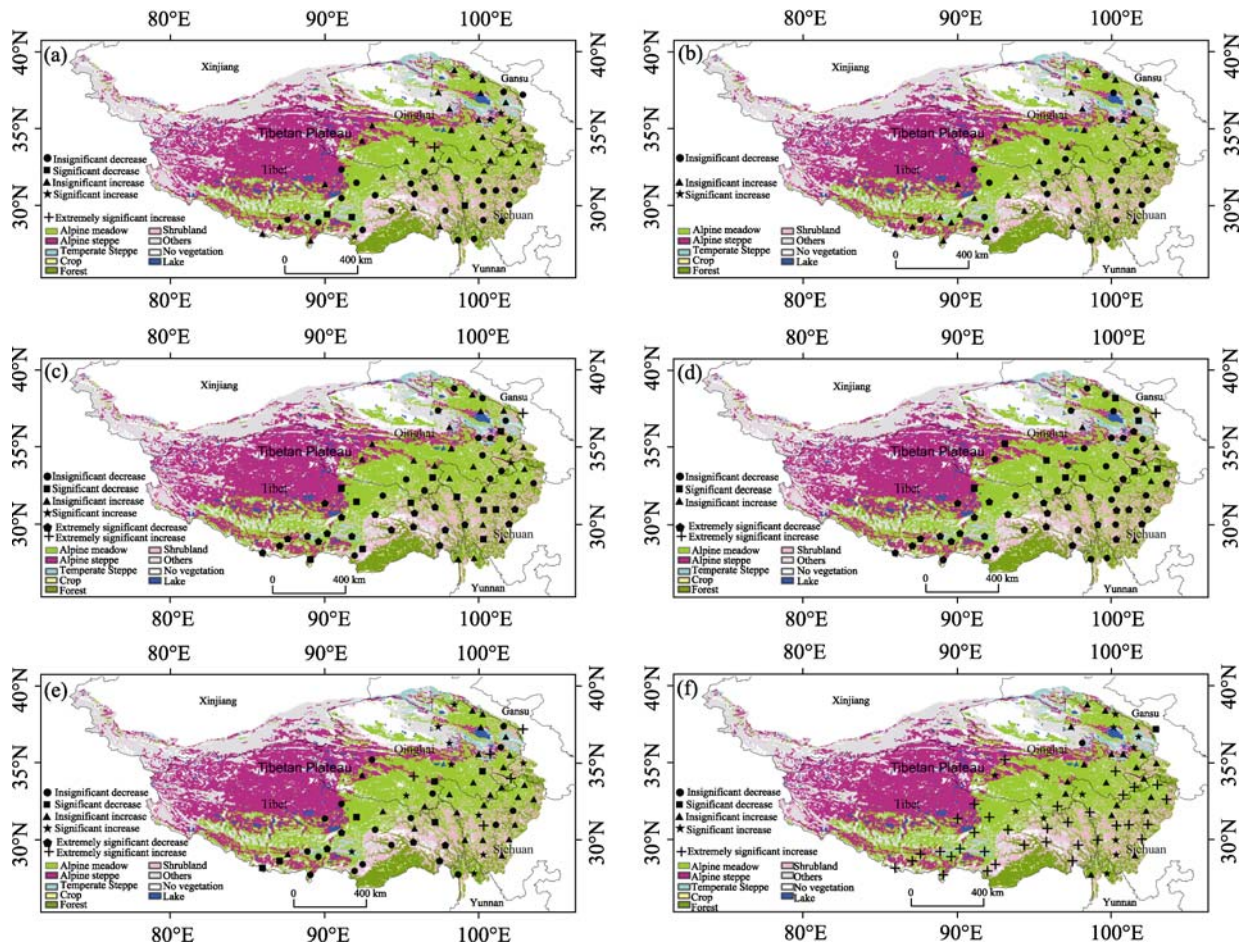
Fig. 7   Annual trends for (a) TP, total precipitation; (b) MAP, maximum precipitation; (c) Ea, average vapor pressure; (d) RH, average relative humidity; (e) MIRH, minimum relative humidity; (f) VPD, average vapor pressure deficit; from 2000 to 2011 at 69 meteorological stations on the Tibetan Plateau.
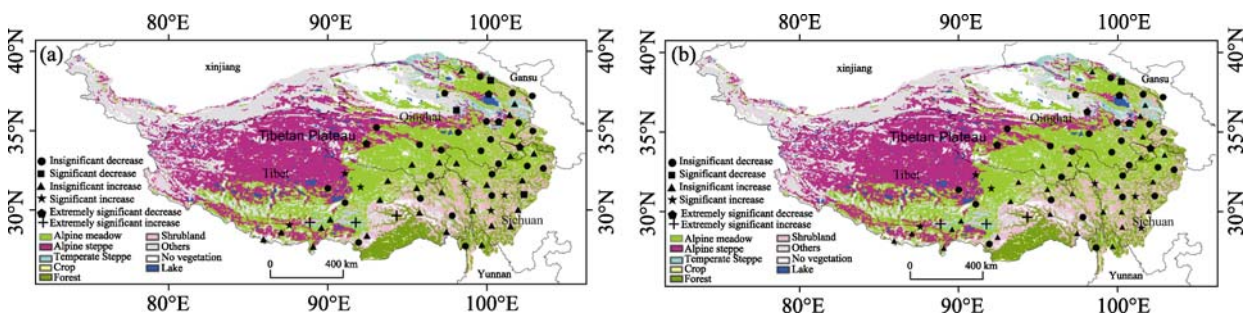

Fig. 8   Annual trends for (a) SP, percentage of sunshine; (b) SH, sunshine hours; from 2000 to 2011 at 69 meteorological stations on the Tibetan Plateau.

Spatially averaged DSI increased as TP increased in alpine meadows, alpine steppes and shrublands (Table 1). Spatially averaged DSI showed a positive correlation with Ea in alpine meadows, forests, and shrublands (Table 1). Spatially averaged DSI decreased as VPD increased, but increased as RH increased in forests and shrublands (Table 1). Spatially averaged DSI showed a positive relationship with MIRH in alpine meadows and shrublands (Table 1). These findings indicate that DSI can mirror the dynamics of water availability at the whole ecosystem scale. However, the degree of correlation between DSI and climate factors related to water availability varied with vegetation type (Table 1). Therefore, clarifying the correlation between DSI and water availability requires taking into consideration the type of ecosystem.
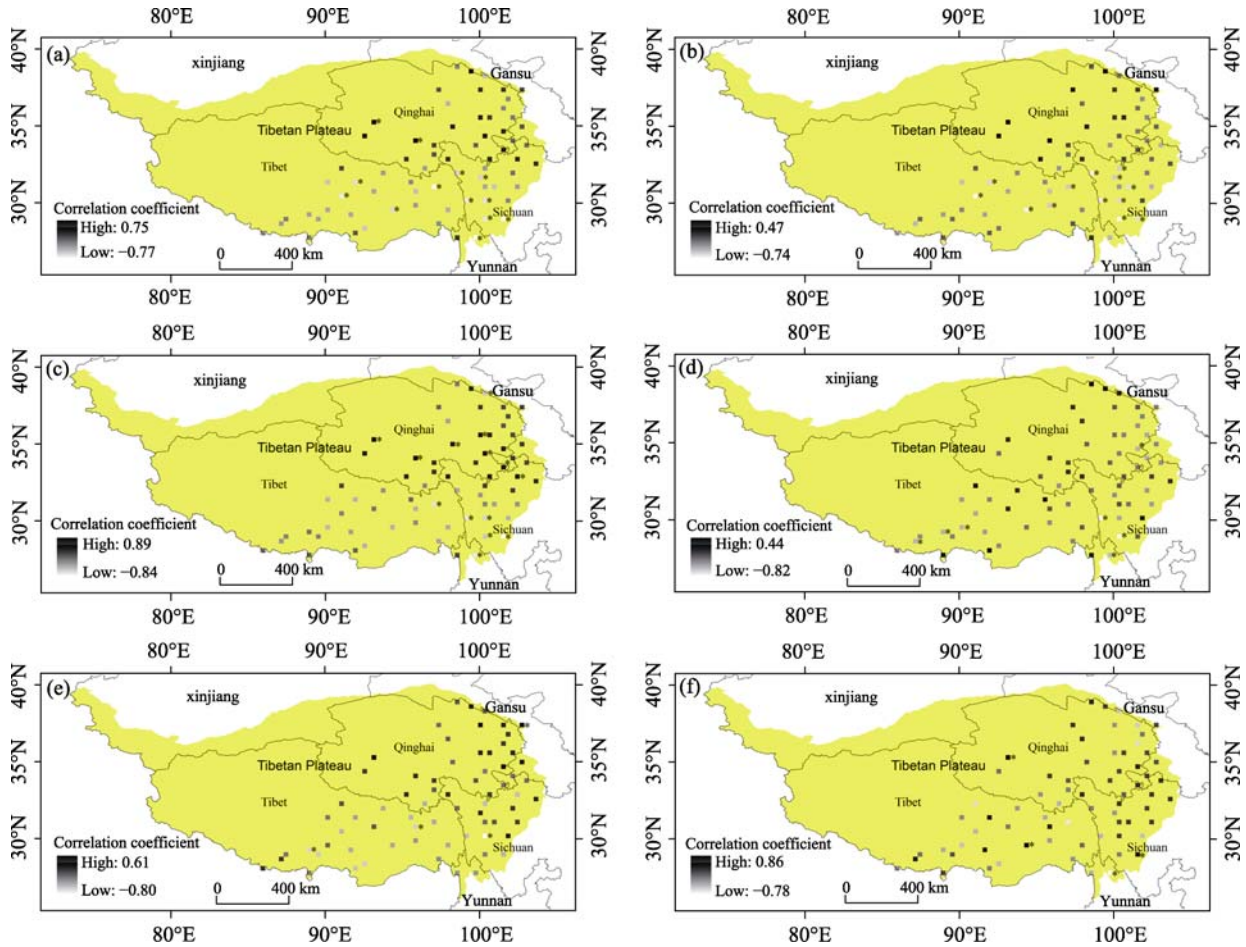
Fig. 9   Correlation coefficients of the drought severity index (DSI) with: (a) Ta, average air temperature; (b) MAT, maximum air temperature; (c) MIT, minimum air temperature; (d) EMAT, extreme maximum air temperature; (e) EMIT, extreme minimum air temperature; (f) WS, average wind speed; from 2000 to 2011 at 69 meteorological stations on the Tibetan Plateau.

Generally, correlations between DSI and climate factors varied among the 69 meteorological stations. At three stations, wind speed was the dominant factor influencing DSI, at 26 stations temperature factors were dominant, at 11 stations precipitation factors were dominant, at 15 stations air humidity factors were dominant, and at 14 stations sunshine factors were dominant. Most stations showed positive correlations between DSI and water availability, and these stations were distributed mainly in the center and east of Tibet, the east and south of Qinghai and the northwest of Sichuan (Fig. 9, Fig.10, Fig.11). A study of the spatial and temporal drought patterns in Tibet from 1981 to 2013, based on the standardized precipitation index (SPI), also showed that the center and east of Tibet experienced a high frequency of severe drought (Yuan et al., 2015).

Most meteorological stations showed negative correlations between DSI and sunshine conditions, and these stations were distributed mainly in the east of Tibet, the south of Qinghai and the northwest of Sichuan. Among this group of stations, ten stations were found to have significant correlations ($P<0.05$), and these station were located in the southeast of Qinghai and the northwest of Sichuan (Fig. 11).

Most stations also showed negative correlations of DSI with MAT and EMAT, and these stations were distributed mainly in the center and east of Tibet, the southeast of Qinghai and the northwest of Sichuan. There were more than ten stations that showed significant correlations of DSI with MAT ($P<0.05$), located in the southeast of Tibet and the northwest of Sichuan (Fig. 9).

More than 50% of the meteorological stations showed negative correlations of DSI with Ta, MIT and EMIT, and these stations were distributed mainly in central and eastern Tibet and the northwest of Sichuan. Five stations showed significant correlations of DSI with Ta and MIT ($P< 0.05$), and these were located in the northwest of Sichuan (Fig. 9). These findings indicate that DSI can mirror water availability at the individual meteorological station scale. Wang et al. (2013) demonstrated that meteorological stations with high sensitivity to change in the dryness index during the growing season were mainly concentrated in the central and eastern parts of the Tibetan Plateau. This finding was based on observational data from ground meteorological stations and MODIS enhanced vegetation index data for the years 2001 to 2010 (Wang et al., 2013). Moreover, both global
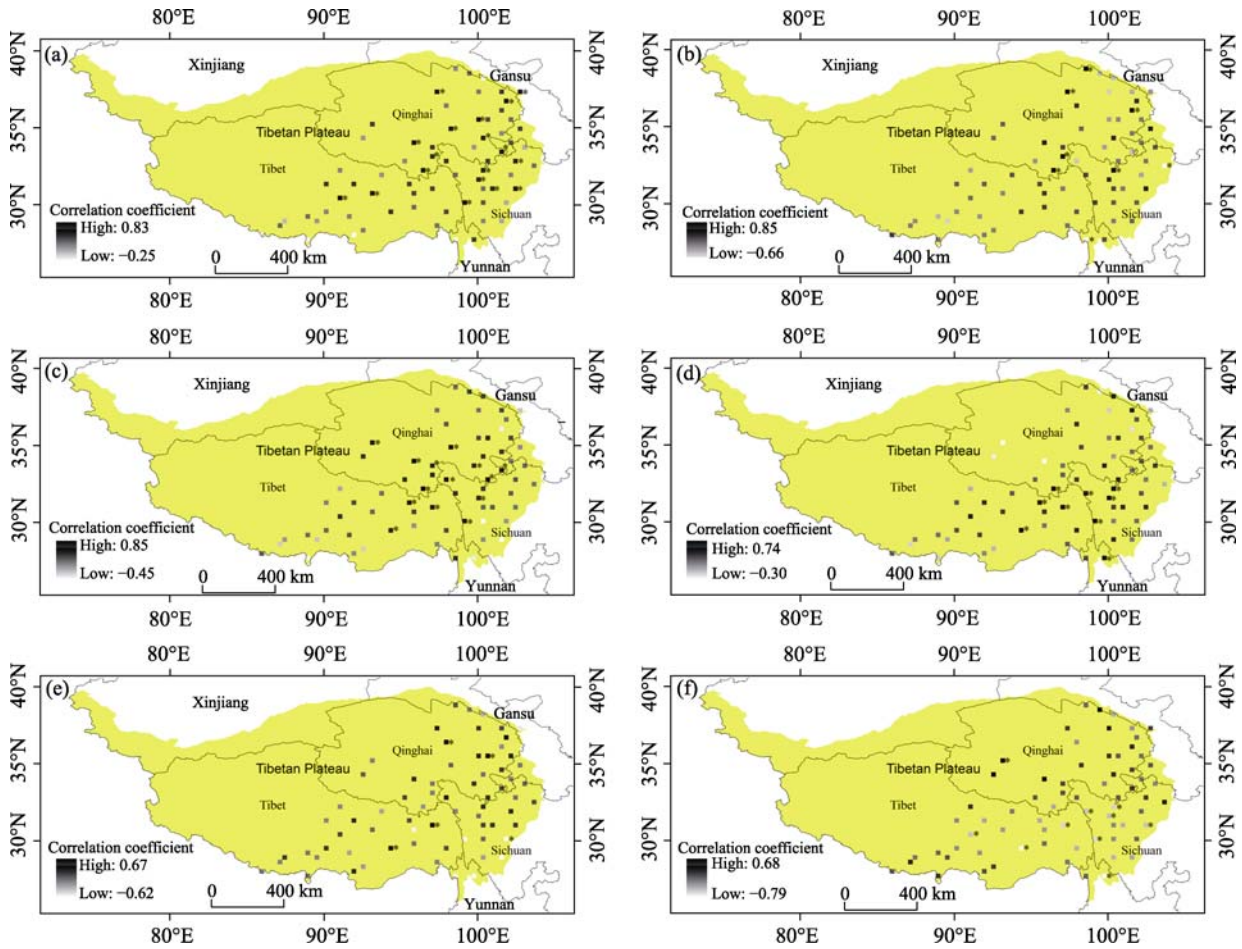
Fig. 10   Correlation coefficients of the drought severity index (DSI) with: (a) TP, total precipitation; (b) MAP, maximum precipitation; (c) Ea, average vapor pressure; (d) RH, average relative humidity; (e) MIRH, minimum relative humidity; (f) VPD, average vapor pressure deficit; from 2000 to 2011 at 69 meteorological stations on the Tibetan Plateau.
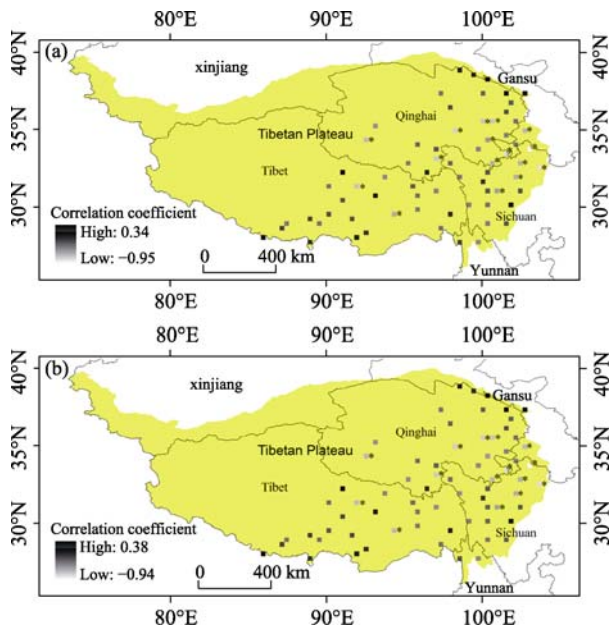

Fig. 11   Correlation coefficients of the drought severity index (DSI) with annual: (a) SP, percentage of sunshine; (b) SH, sunshine hours; from 2000 to 2011 at 69 meteorological stations on the Tibetan Plateau.

warming and the increase in sunshine resulted in drying at most stations. This finding is consistent with previous studies conducted on the Tibetan Plateau (Klein et al., 2004; Shen et al., 2015).

Spatially averaged DSI decreased as Ta, MAT, and EMAT increased in forests and shrublands (Table 1). Spatially averaged DSI also showed a negative correlation with MIT and EMIT in forests (Table 1). These findings indicate that global warming may result in drying at the whole ecosystem scale; this finding is consistent with those of previous studies (Wang et al., 2015; Yu et al., 2019a). Spatially averaged DSI showed a negative correlation with SP and SH in alpine meadows, alpine steppes, croplands, forests and shrublands (Table 1), suggesting that the increase of sunshine may cause drying at the whole ecosystem scale.

4   Conclusions

In this study, we investigated the correlation of DSI with 14 climate factors (including factors for temperature, precipitation, humidity, wind speed, and sunshine) from 2000 to 2011 on the Tibetan Plateau. Our main conclusions are as

follows: 1) spatial DSI averages increased as precipitation and minimum relative humidity increased, but decreased as sunshine increased; 2) The correlation between DSI and climate factors differed due to the changes of the climate factors and the difference of background values among different vegetation types; and 3) The degree of correlation between DSI and climate change was stronger in environments that were colder and drier, and had higher wind speeds and more sunshine. These findings indicate that DSI can mirror the dynamics of water availability regardless of location or ecosystem scale. This study provides a scientific basis for local meteorological departments to implement effective, long-term drought monitoring programs. This is important and has practical significance for agriculture, animal husbandry and human life in alpine regions.

References

Atkinson P M, Dash J, Jeganathan C. 2011. Amazon vegetation greenness as measured by satellite sensors over the last decade. *Geophysical Research Letters*, 38(19): 1–6.

Dai A G. 2011. Drought under global warming: A review. *Wiley Interdisciplinary Reviews–Climate Change*, 2(1): 45–65.

Dai A G. 2013. Increasing drought under global warming in observations and models. *Nature Climate Change*, 3(1): 52–58.

Fu G, Shen Z X. 2016. Environmental humidity regulates effects of experimental warming on vegetation index and biomass production in an alpine meadow of Northern Tibet. *Plos One*, 11(10). DOI: 10.1371/journal. pone.0165643.

Intergovernmental Panel on Climate Change (IPCC). 2013. Summary for Policymakers. In: Stocker T F, Qin D, Plattner G K, et al.(eds.). Climate change 2013: The physical science basis. Contribution of working group I to the fifth assessment report of the intergovernmental panel on climate change. Cambridge: Cambridge University Press.

Kerchove R V D, Lhermitte S, Veraverbeke S, et al. 2013. Spatio-temporal variability in remotely sensed land surface temperature, and its relationship with physiographic variables in the Russian Altay Mountains. *International Journal of Applied Earth Observation & Geoinformation*, 20(2): 4–19.

Klein J A, Harte J, Zhao X Q. 2004. Experimental warming causes large and rapid species loss, dampened by simulated grazing on the Tibetan Plateau. *Ecology Letters*, 7: 1170–1179.

Li L Y, Zhang J, Wu S, et al. 2019. Increasing sensitivity of alpine grasslands to climate variability along an elevational gradient on the Qinghai-Tibet Plateau. *Science of the Total Environment*, 678: 21–29.

Li N, Wang G X, Yang Y, et al. 2011. Plant production, and carbon and nitrogen source pools, are strongly intensified by experimental warming in alpine ecosystems in the Qinghai-Tibet Plateau. *Soil Biology & Biochemistry*, 43(5): 942–953.

Liu D K, Wang J B, Qi S H. 2014. Analysis on dry trend based on moisture index in Qinghai Province in the recent 35 years. *Research of Soil and Water Conservation*, 21(2): 246–250.

Mu Q Z, Zhao M S, Kimball J S, et al. 2013. A remotely sensed global terrestrial drought severity index. *Bulletin of the American Meteorological Society*, 94(1): 83–98.

Seager R, Naik N, Vecchi G A. 2010. Thermodynamic and dynamic mechanisms for large-scale changes in the hydrological cycle in response to global warming. *Journal of Climate*, 23(17): 4651–4668.

Sheffield J, Wood E F, Roderick M L. 2012. Little change in global drought over the past 60 years. *Nature*, 491(7424): 435–438.

Shen Z X, Fu G, Yu C Q, et al. 2014. Relationship between the growing season maximum enhanced vegetation index and climatic factors on the Tibetan Plateau. *Remote Sensing*, 6(8): 6765–6789.

Shen Z X, Li Y L, Fu G. 2015. Response of soil respiration to short-term experimental warming and precipitation pulses over the growing season in an alpine meadow on the Northern Tibet. *Applied Soil Ecology*, 90: 35–40.

Shen Z X, Wang J W, Sun W, et al. 2016. The soil drying along the increase of warming mask the relation between temperature and soil respiration in an alpine meadow of Northern Tibet. *Polish Journal of Ecology*, 64:125–129.

Sun D, Kafatos M. 2007. Note on the NDVI-LST relationship and the use of temperature-related drought indices over North America. *Geophysical Research Letters*, 34(24): 497–507.

Sun J, Cheng G W, Li W P, et al. 2013. On the variation of NDVI with the principal climatic elements in the Tibetan Plateau. *Remote Sensing*, 5: 1894–1911.

Trenberth K E, Dai A G, van der Schrier G, et al. 2014. Global warming and changes in drought. *Nature Climate Change*, 4(1): 17–22.

Wang L, Chen W. 2014. A CMIP5 multimodel projection of future temperature, precipitation, and climatological drought in China. *International Journal of Climatology*, 34(6): 2059–2078.

Wang M, Zhou C P, Wu L, et al. 2013. Wet-drought pattern and its relationship with vegetation change in the Qinghai-Tibetan Plateau during 2001–2010. *Arid Land Geography*, 36(1): 49–56.

Wang S H, Sun W, Li S W, et al. 2015. Interannual variation of the growing season maximum normalized difference vegetation index, MNDVI, and its relationship with climatic factors on the Tibetan Plateau. *Polish Journal of Ecology*, 63(3): 424–439.

Wang S P, Duan J C, Xu G P, et al. 2012. Effects of warming and grazing on soil N availability, species composition, and ANPP in an alpine meadow. *Ecology*, 93: 2365–2376.

Yang X H, Zhuo G, Luo B. 2014. Drought monitoring in the Tibetan Plateau based on MODIS dataset. *Journal of Desert Research*, 34(2): 527–534.

Yuan L, Liu Y, Ma P F. 2015. Analysis of temporal and spatial characteristics of drought in Tibet from 1981 to 2013 based on standardized precipitation index. *China Agronomy Bulletin*, 31(25): 228–234.

Yu C Q, Han F S, Fu G. 2019a. Effects of 7 years experimental warming on soil bacterial and fungal community structure in the Northern Tibet alpine meadow at three elevations. *Science of the Total Environment*, 655: 814–822.

Yu C Q, Wang J W, Shen Z X, et al. 2019b. Effects of experimental warming and increased precipitation on soil respiration in an alpine meadow in the Northern Tibetan Plateau. *Science of the Total Environment*, 647: 1490–1497.

Zhang L, Guo H D, Ji L, et al. 2013. Vegetation greenness trend (2000 to 2009) and the climate controls in the Qinghai-Tibetan Plateau. *Journal of Applied Remote Sensing*, 7(1). DOI: 10.1117/1111.jrs.1117.073572.

Zhong Z M, Shen Z X, Fu G. 2016. Response of soil respiration to experimental warming in a highland barley of the Tibet. *Springer Plus*, 5(137). DOI: 10.1186/s40064–40016–41761–40060.

青藏高原干旱度指数对气候因子变化的响应

王向涛 [1, 2]，张宪洲 [1, 2, 3]，王俊皓 [1, 2]，牛　犇 [1, 2]

1. 中国科学院地理科学与资源研究所，生态系统网络观测与模拟重点实验室，拉萨高原生态试验站，北京　100101；
2. 中国科学院大学，北京　100049；
3. 中国科学院大学资源与环境学院，北京　100190

　　摘　要：在气候变化条件下，干旱如何发生改变仍然没有搞清楚。量化干旱与气候因子之间的关系是预测全球气候变化背景下未来干旱风险发生的关键。本文对 2000–2011 年青藏高原年干旱严重度指数(DSI)与气候因子的相关性进行了研究。空间平均 DSI 随降水量的增加及相对湿度降低而增加，随日照的增加而减少。DSI 与气候因子的相关程度随植被类型的不同而不同。以高寒草甸为例，空间 DSI 平均值与日照百分率(SP)和日照时数(SH)的相关程度($P<0.001$)高于高寒草原($P<0.05$)；在高山草原，空间 DSI 平均值与平均水汽压(Ea)和最低相对湿度(MIRH)的相关性不显著，但在高山草甸为极显著水平或显著水平以上($P<0.05$)。DSI 的变化幅度随温度、降水和水汽压的增加而减小，随风速和日照的增加而增大。因此，要弄清干旱与气候变化的关系，需要进一步考虑青藏高原的生态系统类型及其局地气候。

　　关键词：高寒生态系统；气候变化；干旱；青藏高原